A phase correlation for color images using Clifford algebra

José Mennesson, **Christophe Saint-Jean**, **Laurent Mascarilla**

MIA - Laboratoire Mathématiques, Image et Applications
University of La Rochelle, La Rochelle, France
jose.mennesson@univ-lr.fr [presenter, corresponding]
christophe.saint-jean@univ-lr.fr, laurent.mascarilla@univ-lr.fr

1 Introduction

This article is based on a recent development of a generalization of the Fourier transform. A color Clifford-Fourier transform[1] using geometric algebra is considered to process color images. This transform, defined by Batard *et al.*, generalizes the classical Fourier transform to $L^2(\mathbb{R}^m;\mathbb{R}^n)$ functions. It avoids a marginal processing that is generally applied in color image processing. From this advance, a new color phase correlation is defined and appears highly relevant for several applications, specifically in the image classification field.

2 Clifford Fourier transform for color images

In [1], Batard *et al.* have proposed a definition of the Fourier transform for the $L^2(\mathbb{R}^m;\mathbb{R}^n)$ functions. It has been demonstrated that the previous generalizations of the Fourier transform for color image, i.e. the hyper-complex Fourier transform of Sangwine and Ell [4] and the Biquaternionic Fourier Transform of Pei et al.[9], are particular cases of their proposal. Because of the domain of our application (color image processing), only the Clifford Fourier transform defined from morphisms from $\mathbb{R}^2$ to $Spin(3)$ is used. Its definition for color images is :

$$\widehat{f_B}(u,v) = \int_{\mathbb{R}^2} e^{\frac{(ux+vy)}{2}B}\ f_{\|B}(x,y)\ e^{-\frac{(ux+vy)}{2}B} dxdy + \int_{\mathbb{R}^2} e^{\frac{(ux+vy)}{2}I_4 B}\ f_{\perp B}(x,y)\ e^{-\frac{(ux+vy)}{2}I_4 B} dxdy \tag{1}$$

where B is a bivector of $\mathbb{R}_{4,0}$ which parametrizes the analysis direction, $f_{\|B}$ (resp. $f_{\perp B}$) is the projection of f on the plane generated by B (resp. $I_4 B$).

It is obvious that this formula permits to process the color Fourier transform easily and efficiently thanks to two FFT 2D on $f_{\perp B}$ and $f_{\|B}$.

Note that a unit bivector B can be obtained from the geometric product of two unit orthogonal vectors. In this article, the bivector is chosen as being $C \wedge e_4$ where C is a user-defined color. Obviously, an inverse transform exists and it is denoted by $\breve{f_B}$ [1].
From this Clifford-Fourier transform, we have developed two image recognition methods : the Generalized Fourier Descriptors ($GCFD$) [6] and the Phase Correlation defined in the following section.

3 Phase Correlation for color images

In the literature, the phase correlation [10] is a well-established method that is used for a lot of applications such as image recognition, video stabilization, motion estimation, stereo disparity analysis, vector flow analysis [3] ... It is defined for two grayscale images f and g as :

$r(x,y) = \check{R}(u,v)$ where R is the so-called "cross-power spectrum" $R(u,v) = \dfrac{\widehat{f}(u,v)\ \widehat{g}(u,v)^*}{|\widehat{f}(u,v)||\widehat{g}(u,v)^*|}$

with operator * the usual complex conjugate. The visualization of r as an image reveals a peak corresponding to the best translation estimate between the two images : this is justified by the "*shift theorem*" of the Fourier transform [3]. The value of this peak is used as a correlation score assessing the goodness of the matching between the two images and is denoted by

$$\rho = \max_{x,y} r(x,y)$$

Hopefully, a phase correlation for color images can supply more information than the one computed on gray level images and should give a better translation estimate. Previously, Moxey *et al.* [7] defined an hypercomplex phase correlation for color image based on the hypercomplex Fourier transform. In that case, the image is decomposed into its projection on the luminance and the chrominance axis. In the color Clifford-Fourier transform framework we define a color phase correlation depending on a bivector B. From equation (1), it is obvious that the color Clifford-Fourier transform can be decomposed as :

$$\widehat{f_B}(u,v) = \widehat{f_{\|B}}(u,v) + \widehat{f_{\perp B}}(u,v)$$

From this, identifying $\widehat{f_{\|B}}$ and $\widehat{f_{\perp B}}$ to two distinct complex images, two cross-power spectra for two color images f and g are defined :

$$R_{\|B}(u,v) = \frac{\widehat{f_{\|B}}(u,v)\ \widehat{g_{\|B}}(u,v)^*}{|\widehat{f_{\|B}}(u,v)||\widehat{g_{\|B}}(u,v)^*|} \quad , \quad R_{\perp B}(u,v) = \frac{\widehat{f_{\perp B}}(u,v)\ \widehat{g_{\perp B}}(u,v)^*}{|\widehat{f_{\perp B}}(u,v)||\widehat{g_{\perp B}}(u,v)^*|}$$

By taking the inverse Fourier transform of $R_{\|B}$ and $R_{\perp B}$, the phase correlation of the parallel and the orthogonal part of the image (denoted $r_{\|B}$ and $r_{\perp B}$) are obtained. This is exemplified on Figure 1 with the two correlation scores, $\rho_{\|B}$ and $\rho_{\perp B}$. One can see the peak representing the exact translation processed between the two images. For an image classification purpose a single correlation score is preferred and some proposals to fuse these two values are examined in the application section. A better way should be to directly define the correlation score on $\widehat{f_B}$. This can be done taking the cosine of the angle between the two multi-vectors $\widehat{f_B}(u,v)$ and $\widehat{g_B}(u,v)$ (see [5] page 14):

$$R_B(u,v) = \cos(\widehat{f_B}(u,v), \widehat{g_B}(u,v)) = \frac{\widehat{f_B}(u,v) * \widehat{g_B}^{\dagger}(u,v)}{|\widehat{f_B}(u,v)||\widehat{g_B}(u,v)|}$$

where † is the reverse and $*$ is the Hestenes scalar product. The inverse Fourier transform of this complex image produces two symmetric peaks, due to the cosine, which have the same magnitude. Then the same previous calculi also apply :

$$r_B(x,y) = \check{R_B}(u,v), \text{ and } \rho_B = 2 \times \max_{x,y} r_B(x,y) \tag{2}$$

It can be checked on Figure 1, that the color correlation score ρ_{B_r}, where B_r[1]is $red \wedge e_4$, is the highest. This argues that considering color increases the correlation score between two objects of the same color.

[1]In the following, this notation is used for $B_g = green \wedge e_4$, and so on for *blue*, $\mu = rgb(127,127,127)$ or any given color C

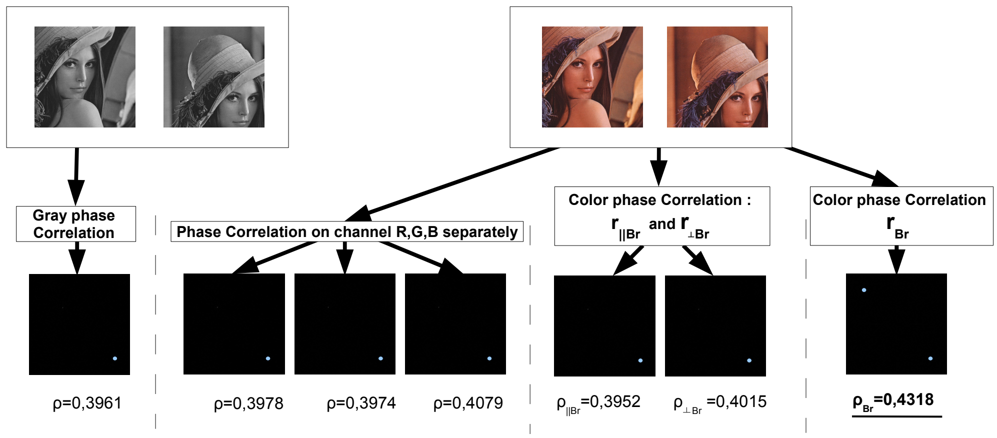

Figure 1: Correlation scores ρ (resp. $\rho_{\|B_r}$, $\rho_{\perp B_r}$, ρ_{B_r}) on grayscale (resp. color) Lena

Results in Table 1 confirm our previous observations. On the one hand, $\rho_{\perp B}$ and $\rho_{\|B}$ are equal to 1 or NaN[2] independently to the bivector B and C_2 choice. On the other hand, ρ_B is lower than 1 depending on C_2 and B: similarly shaped objects of different colors are less similar and lowest scores are obtained by taking B equals to C_1.

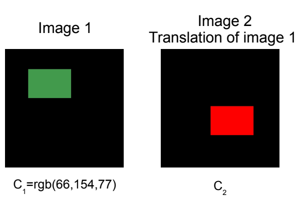

	B_μ			B_r			B_{C_1}		
C_2	$\rho_{\|B_\mu}$	$\rho_{\perp B_\mu}$	ρ_{B_μ}	$\rho_{\|B_r}$	$\rho_{\perp B_r}$	ρ_{B_r}	$\rho_{\|B_{C_1}}$	$\rho_{\perp B_{C_1}}$	$\rho_{B_{C_1}}$
$rgb(66,154,77) = C_1$	1	1	1	1	1	1	1	NaN	1
$rgb(66,0,0)$	1	1	0.36	1	NaN	0.36	1	NaN	0.36
$rgb(0,154,0)$	1	1	0.84	NaN	1	0.84	1	NaN	0.84
$rgb(0,0,77)$	1	1	0.42	NaN	1	0.42	1	NaN	0.42
$rgb(119,119,119) = \mu$	1	NaN	0.93	1	1	0.93	1	NaN	0.93

Table 1: Correlation scores between image 1 and 2 for various choices of C_2 and B. From image 1 to 2, the rectangle has color changed from $C_1 = rgb(66,154,77)$ to C_2 and a translation is applied.

4 Application to image classification

To obtain a single similarity value from $\rho_{\|B}$ and $\rho_{\perp B}$, the most immediate aggregation function is the usual mean, the resulting score is denoted $\rho^{\text{mean}}_{\|B,\perp B}$. However, this score depends on the choice of the bivector B. Then, two distinct classification processes can be done : the first one relies on the arbitrary choice of a unique bivector for the whole dataset while the second determines some ad-hoc bivector for each request image depending on its hue histogram. In both cases, phase correlation is used as a criterion for the "most similar" rule. This method improves the discrimination between two objects which have the same shape but not the same color.

In order to assess the classification performance of these two methods, a comparison with a method based on Generalized Color Fourier descriptors ($GCFD$) [6] is provided. These descriptors are defined from (grayscale) Generalized Fourier Descriptors (GFD) introduced by Smach *et al.* [11] and the Clifford-Fourier transform [1]. It must be emphasized that, by construction, GFD and $GCFD$ are invariant with respect to the action of group M_2, *i.e.* translations and rotations. Previous experiments on well-known databases [6] have shown that the $GCFD$ give better recognition rates than the (grayscale) GFD computed marginally on the R,G, and B planes. Using a 1-NN classifier, we obtain an error of 0.74% for the 128 $GCFD$

[2] NaN denotes that the correlation score cannot be calculated because Fourier transform is null (e.g. parallel part of a red image for a blue bivector is null)

descriptors on the COIL-100 database [8]. On the same database $\rho^{\text{mean}}_{\|B_r,\perp B_r}$ yields an error of 9%. When c_i corresponds to the principal mode of the hue histogram $\rho^{\text{mean}}_{\|B_i,\perp B_i}$ gives an error of 7.22 %.

The superiority of descriptors $GCFD$ was predictable from a theoretical point of view, because of the quality of the used classifier and of the size of descriptors. However, the results of the proposed methods are quite encouraging knowing that they are based on a single number. Let us also remark that these methods can be fairly improved by transforming the images in log-polar domain to achieve a rotation and scale invariance. In the same way, various criteria for fusing the $\rho_{\|B}$ and $\rho_{\perp B}$ should to be examined (e.g. the maximum, the minimum) and compared to the classification rate using the correlation as calculated by ρ_B, *i.e.* by using the equation (2). Tests on $r_B(x, y)$ are ongoing as well as experiments on other bases. An improvement will also be done by using a similarity-based SVM [2] allowing the use of our criteria with this classifier and compete with Fourier Descriptors.

References

[1] T. Batard, M. Berthier, and C. Saint-Jean. Clifford fourier transform for color image processing. In E. Bayro-Corrochano and G. Scheuermann Eds, editors, *Geometric Algebra Computing in Engineering and Computer Science*, chapter 8, pages 135–161. Springer Verlag, 2010.

[2] Y .Chen, K. E. Garcia, M. R. Gupta, A. Rahimi, and L. Cazzanti. Similarity-based classification: Concepts and algorithms. *J. Mach. Learn. Res.*, 10:747–776, 2009.

[3] J. Ebling and G. Scheuermann. Clifford fourier transform on vector fields. *IEEE Transactions on Visualization and Computer Graphics*, 11:469–479, 2005.

[4] T. A. Ell and S. J. Sangwine. Hypercomplex fourier transforms of color images. *IEEE Transactions on Image Processing*, 16(1):22–35, 2007.

[5] D. Hestenes and G. Sobczyk. *Clifford Algebra to Geometric Calculus.* Reidel and Dordrecht, 1984.

[6] J. Mennesson, C. Saint-Jean, and L. Mascarilla. De nouveaux descripteurs de fourier géométriques pour l'analyse d'images couleur. In *Actes de la conférence RFIA 2010 Reconnaissance des Formes et Intelligence Artificielle*, pages 599–606, Caen France, 01 2010.

[7] C. E. Moxey, S. J. Sangwine, and T. A. Ell. Color-grayscale image registration using hypercomplex phase correlation. In *ICIP (2)*, pages 385–388, 2002.

[8] S. A. Nene, S. K. Nayar, and H. Murase. Columbia object image library (coil-100), 1996. Technical Report CUCS-006-96.

[9] S.-C. Pei, J.-H. Chang, and J.-J. Ding. Commutative reduced biquaternions and their fourier transform for signal and image processing applications. *IEEE Transactions on Signal Processing*, 52(7):2012–2031, 2004.

[10] S. B. Reddy and B. N. Chatterji. An fft-based technique for translation, rotation, and scale-invariant image registration. *IEEE Transactions on Image Processing*, 5(8):1266–1271, August 1996.

[11] F. Smach, C. Lemaître, J. P. Gauthier, J. Miteran, and M. Atri. Generalized fourier descriptors with applications to objects recognition in svm context. *Journal of Mathematical Imaging and Vision*, 30(1):43–71, 2008.